ISSN: 2688-8645

Study on Wind Speed Distribution Law of Mine Roadway Section under Different Conditions

Rui Sun[1, 2]

[1]Chongqing Research Institute of China Coal Technology and Industry Group, Chongqing 400037, China

[2]State Key Laboratory of Coal Mine Disaster Prevention and Control, Chongqing 400037, China

Abstract

Ventilation is the cornerstone of coal mine safety production, and accurate monitoring of ventilation parameters is the basic guarantee for ventilation technology decision-making. Aiming at the problem that the accuracy of wind speed monitoring in coal mine roadway is difficult to meet the needs of decision-making, this paper studies the position relationship between the average wind speed line and the roadway wall surface by combining theoretical calculation and numerical simulation, and simulates the wind speed distribution law of typical roadway section. The main factors affecting the distribution of wind speed in roadway section include roadway section shape, section size, support form, wind speed, facilities and equipment status, etc. The expression of the position relationship between the average wind speed line of the rectangular and semi-circular arch roadway section and the roadway wall surface is $y=e^{\ln a-1.5}$. Through 25 groups of model simulation, the wind speed distribution law of different types of roadway sections under different conditions is obtained: the wind speed contour is basically parallel to the roadway wall. The wind speed gradient near the roadway wall is large, and the wind speed gradient in the middle of the roadway is small. The thickness of the boundary layer decreases with the increase of wind speed.

Keywords

Mine Ventilation; Average Wind Speed; Wind Speed Contour; Wind Speed Distribution; Numerical Simulation.

1. Introduction

The geological conditions for the occurrence of coal resources in China are complex, and most mines are mainly operated by underground mining. The threat of disasters is relatively serious, and coal mine safety accidents occur from time to time [1-3]. The coal mine production system includes subsystems such as excavation, coal mining, electromechanical, transportation, and ventilation. Among them, a stable and reliable mine ventilation system is the fundamental guarantee for its safe and efficient production [4-6]. In the production process of coal mines, due to the constantly changing working environment and tunnel conditions, in order to accurately calculate tunnel ventilation parameters, reasonably arrange ventilation systems, improve the effectiveness of monitoring and control, and achieve safety risk prevention and control, it is necessary to study and master the distribution characteristics of wind speed field in different types of tunnels underground, among which the tunnel section is an important factor affecting wind speed distribution.

The common types of cross sections in mine tunnels are rectangular or trapezoidal, arched or circular. Many scholars at home and abroad have conducted extensive theoretical and experimental research on the distribution patterns of airflow in different tunnel sections. Lu

ISSN: 2688-8645

Guangli et al. [7] used the Prandtl theory and combined it with CFD simulation to analyze the wind speed distribution patterns in rectangular, semi-circular arch, and trapezoidal tunnel sections, and tested the applicability of the Prandtl theory in the turbulent core area. Zhou Xihua et al. [8] studied the distribution pattern of wind speed on circular cross-sections through indoor experiments and numerical simulations, and obtained the proportion coefficient of the conversion relationship between wind speed at cross-sections and average wind speed. Wang Hanfeng [9] used Fluent software to numerically simulate the wind speed on the axis of rectangular and semi-circular arch tunnel sections, and found the point where the wind speed value is equal to the average wind speed of the section. This provides support for the precise monitoring of ventilation parameters such as tunnel wind speed and air volume using wind speed sensors in mines. Song Ying et al. [10-11] conducted experiments on wind speed in semi-circular arch, rectangular, and trapezoidal tunnel sections using Laser Doppler Velocimetry, and combined it with numerical simulation to analyze the distribution pattern of wind speed in tunnel sections. Other scholars [12-15] have also conducted extensive research on the distribution of wind speed in tunnels, mainly including the changes in wind speed distribution caused by sudden changes in tunnel section size, the influence of human factors on wind speed measurement, the distribution characteristics of wind speed in trapezoidal tunnels, the application of maximum wind speed method, and the single point measurement method of average wind speed in tunnels based on numerical simulation.

At present, there is relatively little theoretical research on the location of the average wind speed on the cross-section of the tunnel. Through a combination of various research methods, it has been found that the average wind speed line is a fixed position within the cross-section, but no theoretical derivation has been made for the specific location [16-17]. Therefore, based on previous research, the research topic is the distribution of wind speed on the cross-section of rectangular and semi-circular arched tunnels, theoretical analysis and numerical simulation are combined to obtain the theoretical relationship between point wind speed and average wind speed, as well as the position relationship between average wind speed line and shaft wall. And numerical simulation is used to simulate the distribution of airflow field in rectangular and semi-circular arched tunnels.

2. Theoretical Model of the Relationship between the Average Wind Speed Line and the Distance from the Wall of a Mine Roadway

By analyzing the theories and principles of tunnel wind speed distribution, including scholars such as B.H Voronin, Wang Yingmin, Ji Chaosong and Prandtl, combined with the given tunnel wind speed distribution function and average wind speed calculation formula, it is easy to see that the distribution of tunnel wind speed is mainly affected by the friction resistance coefficient of the tunnel (α), the distance between the measuring point and the centerline of the tunnel (r), as well as the influence of the shape and size of the tunnel cross-section. The friction resistance coefficient of the tunnel (α), the calculation is as follows:

$$\alpha = \lambda\rho/8 \quad (1)$$

$$\lambda = 1/(1.74+2\lg(d/\varepsilon))^2 \quad (2)$$

In the formula: ρ *i*s the air density, kg/m^3; λ is the dimensionless coefficient along the resistance coefficient; d is the equivalent diameter of the tunnel, which is related to the shape and size of the tunnel, m; ε is the absolute roughness of the tunnel wall is related to the support form and forming condition of the tunnel, m.

It can be seen that factors such as air density, tunnel roughness, tunnel section shape, and tunnel section size all have a certain impact on the friction resistance coefficient. The wind speed at a certain point in the tunnel is related to the air supply volume of the tunnel. In addition, the tape machines, air ducts, and various pipelines placed in the tunnel will have an impact on

ISSN: 2688-8645

the distribution of wind speed in the tunnel. In summary, for actual tunnel conditions, the distribution of wind speed in tunnel sections is mainly influenced by factors such as tunnel section shape, section size, tunnel air supply, section forming quality, support form, and internal facilities of the tunnel.

2.1. Location of Average Wind Speed Line on Rectangular Cross-section

Based on the Boussinesk theory and Prandtl turbulence theory, a calculation model for the distribution pattern of wind speed in rectangular tunnels was established, as shown in Figure 1. The two closed dashed lines in the figure represent the wind speed contour lines at a distance dy, which are parallel to the tunnel wall. The wind speed corresponding to any point in the figure is:

$$\mu = \sqrt{\frac{\alpha \bar{v}^{-2}}{\rho}} \frac{1}{k} \ln y + C \tag{3}$$

In the formula: μ is wind speed at any point, m/s; $\bar{v}$ is average wind speed of tunnel section, m/s; ρ is air density in the tunnel, kg/m^3; y is the distance from any flow layer in the tunnel to the tunnel wall, m; α is the coefficient of frictional resistance; k is mixed length coefficient; C is an integral constant.

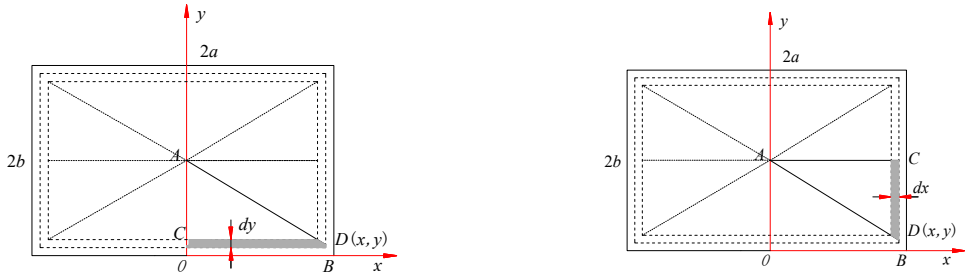

(a) to the top and bottom of the tunnel (b) to the left and right sides of the tunnel

Figure 1. Calculation model for the average wind speed line position in rectangular tunnels

In a rectangular tunnel, the airflow corresponding to the AOB area Q_1 is:

$$Q_1 = \int_0^b (\sqrt{\frac{\alpha \bar{v}^{-2}}{\rho}} \frac{1}{k} \ln y + C)(a - \frac{a}{b} y) dy \tag{4}$$

In the formula: a is half of the length of the rectangular roadway; b is half the width of a rectangular roadway.

According to the symmetry of the rectangular tunnel, the airflow of the entire cross-section of the rectangular tunnel Q is:

$$Q = 8Q_1 = 4afb \ln b - 6afb + 4abC \tag{5}$$

From the relationship between air volume and cross-sectional area of the tunnel, it can be concluded that the average wind speed of the rectangular section in Figure 1 (a) is:

$$\bar{v} = \frac{Q}{4ab} \tag{6}$$

Assuming that the wind speed at any point in the tunnel is the average wind speed of the tunnel, the distance from the average wind speed line of the rectangular tunnel section to the top and bottom plate after simplification is:

$$y = e^{\ln b - 1.5} \tag{7}$$

Similarly to Figure 1 (a), the distance from the average wind speed line of the cross-section of the roadway to the left and right sides of the roadway can be obtained as:

$$x = e^{\ln a - 1.5} \tag{8}$$

ISSN: 2688-8645

Formulas (7) and (8) represent the relationship between the average wind speed line and the tunnel wall. From the expression, it can be seen that the position of the average wind speed line in a rectangular tunnel is only related to the tunnel size and is independent of other main control factors. Similarly, through theoretical derivation of the average wind speed line for rectangular tunnels with semi-circular arches, trapezoids, and circular cross-sections, consistent conclusions have been drawn. Therefore, the position of the average wind speed line in the roadway is only related to the size of the roadway and is not related to other controlling factors.

2.2. Location of Average Wind Speed Line on the Cross-section of a Semi-circular Arch

Due to the fact that the cross-section of a semi-circular arch roadway consists of a rectangular cross-section and a semi-circular cross-section directly on that cross-section, and the distance from the average wind speed line to the two sides of the roadway and the distance from the cross-section to the bottom of the roadway are the same as the calculation formula for a rectangular roadway, only the distance from the semi-circular arc part of the average wind speed line of the semi-circular arch roadway cross-section to the top plate of the semi-circular arch roadway cross-section contour line is derived. The contour line of the semi-circular arched roadway section and the top plate are semi-circular arc lines, and the diameter of the semi-circular part is equal to the width of the tunnel waistline 2a, and the center of the circle coincides with the center of the top edge line of the rectangular part.

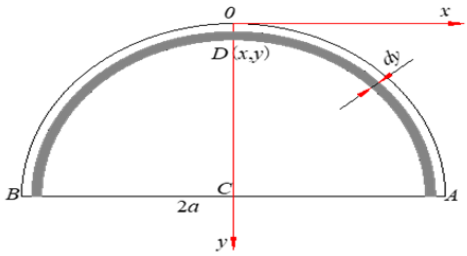

Figure 2. Calculation model for wind speed distribution on the cross-section of a semi-circular arch roadway

As shown in Figure 2, a calculation model for the distribution law of wind speed on the cross-section of a semi-circular arch roadway is established, with the vertex of the arc as the coordinate origin. A Cartesian coordinate system is established, and the black filled area in the figure is the area between two wind contour lines. Based on the Boussinesk theory and Prandtl turbulence theory, an integral expression for the air flow corresponding to a semi-circular arch tunnel is established. The expression for the air flow corresponding to a semi-circular arch tunnel (Q) is obtained as follows:

$$Q = \pi \int_0^a (f \ln y + C)(a - y)dy = \frac{1}{2}\pi a^2 f \ln a - \frac{3}{4}\pi a^2 f + \frac{1}{2}\pi a^2 C \tag{9}$$

According to the relationship between air volume and cross-sectional area of the roadway, the average wind speed corresponding to a semi-circular arch roadway is:

$$\bar{v} = f\ln a\text{-}1.5f\text{+}C \tag{10}$$

The distance y between the average wind speed line and the wall of the semi-circular arch tunnel can be calculated as:

$$y = e^{\ln a\text{-}1.5} \tag{11}$$

Through the theoretical derivation above, the general expression for calculating the air volume of a semi-circular arch tunnel and the expression for the relationship between the average wind

ISSN: 2688-8645

speed line and the tunnel wall surface have been obtained. It can be seen that in the semi-circular arch roadway, the position of the average wind speed line is only related to the size of the roadway and is independent of other control factors.

3. Numerical Simulation of the Distribution Law of Wind Speed on the Cross-Section of Tunnels

3.1. Geometric Models

Using COMSOL Multiphysics numerical simulation software, select the steady-state analysis under the k-ε turbulence model directory in the software for solution. All examples in this study were set using turbulent kinetic energy and turbulent dissipation rate, and their values were determined based on the actual situation of the examples. The rough wall is set using a logarithmic wall function. Based on on-site testing experience, 3 rectangular tunnel sizes and 2 semi-circular arch tunnel sizes, 5 sets of inlet wind speeds, and 2 support types corresponding to tunnel types were selected for simulation calculations. A total of 5 models and 25 sets of simulation tests were conducted. The simulation scheme is shown in Table 1.

Table 1. Simulation scheme

Section type	Section size (width×height)/m×m	Inlet velocity /(m.s^{-1})	Number of scheme groups
Rectangle	4×3/5×3.5/6×4	0.8/2/4/6/8	15
Semicircular arch	4×3/4.5×3.3	0.8/2/4/6/8	10

Establish geometric models for different cross-sectional sizes of semicircular arches and rectangular tunnels, each with a length of 100m. The geometric models for this numerical simulation are shown in Figure 3.

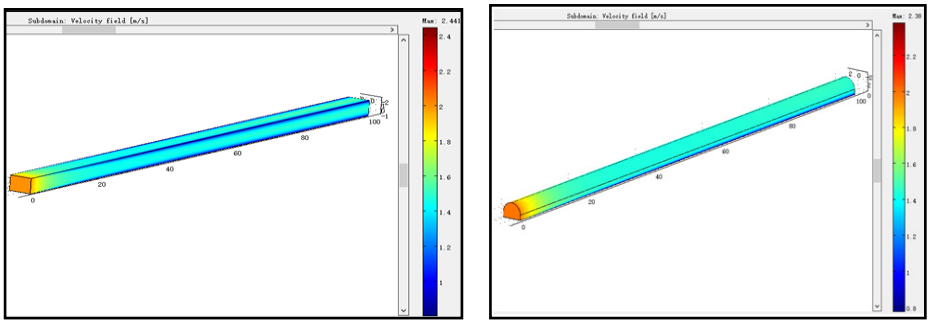

(a) Model of rectangular tunnel model (b) Model of semicircular arch roadway

Figure 3. Geometric models

3.2. Basic Parameters for Simulation

(1) Rectangular roadway

The rectangular tunnels simulate the wind speed distribution patterns of 15 schemes in the anchor net support state, including three cross-sectional dimensions of the tunnel: 4m wide × 3m high, 5m wide × 3.5m high, and 6m wide × 4m high, with 5 inlet wind speeds. The specific schemes and parameters are shown in Table 2.

ISSN: 2688-8645

Table 2. Basic parameters for simulating rectangular tunnels

Section size/m×m	Wind speed / m.s^{-1}	Hydraulic diameter /m	V/ m^2.s^{-1}	Re	I %
4m wide × 3m high	0.8	3.43	14.4×10^{-6}	1.91×10^{5}	3.51
	2	3.43	14.4×10^{-6}	4.76×10^{5}	3.12
	4	3.43	14.4×10^{-6}	9.53×10^{5}	2.86
	6	3.43	14.4×10^{-6}	1.43×10^{6}	2.72
	8	3.43	14.4×10^{-6}	1.91×10^{6}	2.62
5m wide × 3.5m high	0.8	4.12	14.4×10^{-6}	2.29×10^{5}	3.42
	2	4.12	14.4×10^{-6}	5.72×10^{5}	3.05
	4	4.12	14.4×10^{-6}	1.14×10^{6}	2.81
	6	4.12	14.4×10^{-6}	1.72×10^{6}	2.66
	8	4.12	14.4×10^{-6}	2.28×10^{6}	2.57
6m wide × 4m high	0.8	4.81	14.4×10^{-6}	2.67×10^{5}	3.36
	2	4.81	14.4×10^{-6}	6.67×10^{5}	2.99
	4	4.81	14.4×10^{-6}	1.33×10^{6}	2.75
	6	4.81	14.4×10^{-6}	2.00×10^{6}	2.61
	8	4.81	14.4×10^{-6}	2.67×10^{6}	2.51

(2) Semicircular arch roadway

The semicircular arch roadway simulates the wind speed distribution patterns of the roadway with two cross-sectional sizes of 4m wide × 3m high, 4.5m wide × 3.3m high, as well as 5 inlet wind speeds. There are a total of 10 schemes under anchor spray support. The specific simulation parameters are shown in Table 3.

Table 3. Basic parameters for simulating semi-circular arch tunnels

Section size/m×m	Wind speed / m.s^{-1}	Hydraulic diameter /m	V/ m^2.s^{-1}	Re	I %
4m wide × 3m high	0.8	3.44	14.4×10^{-6}	7.17×10^{4}	3.96
	2	3.44	14.4×10^{-6}	1.91×10^{5}	3.50
	4	3.44	14.4×10^{-6}	4.78×10^{5}	3.12
	6	3.44	14.4×10^{-6}	9.56×10^{5}	2.86
	8	3.44	14.4×10^{-6}	1.43×10^{6}	2.72
4.5m wide × 3.3m high	0.8	3.82	14.4×10^{-6}	7.96×10^{4}	3.90
	2	3.82	14.4×10^{-6}	2.12×10^{5}	3.45
	4	3.82	14.4×10^{-6}	5.31×10^{5}	3.08
	6	3.82	14.4×10^{-6}	1.06×10^{6}	2.82
	8	3.82	14.4×10^{-6}	1.59×10^{6}	2.69

ISSN: 2688-8645

4. Simulation Results and Analysis

4.1. The Distribution Characteristics of Airflow Field on the Cross-section of the Tunnel

According to the simulation plan, contour maps of velocity distribution on different cross-sections of the tunnel were simulated. In order to facilitate comparative analysis, contour maps of three wind speed values, namely 0.8m/s, 4.0m/s, and 8.0m/s were selected. Some of the results are shown in Figures 4~5. In general, there will be vortices appearing in the airflow field at the inlet section. In establishing a simplified velocity model, considering avoiding the influence of eddy currents in the tunnel flow field, a cross-sectional data at a distance of 50m from the tunnel entrance is selected as the basis. At this time, the airflow velocity field on the cross-section remains basically unchanged and reaches a fully developed state.

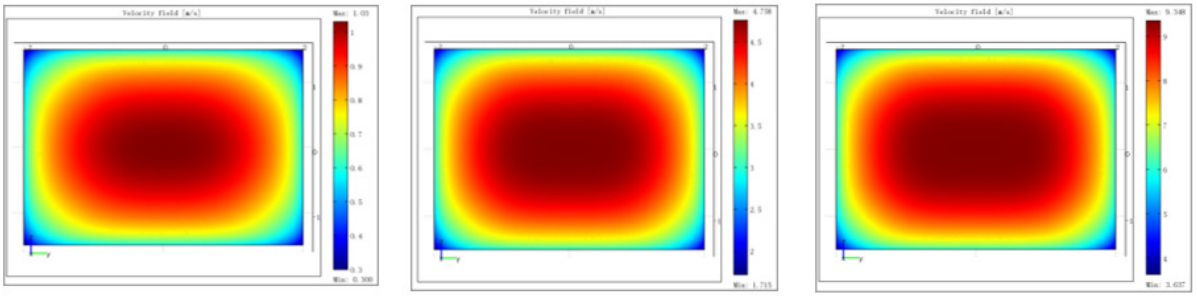

(a)Entrance wind speed of 0.8m/s (b)Entrance wind speed of 4m/s (c)Entrance wind speed of 8m/s

Figure 4. Contour map of velocity distribution at different inlet wind speeds in a rectangular tunnel (4m×3m)

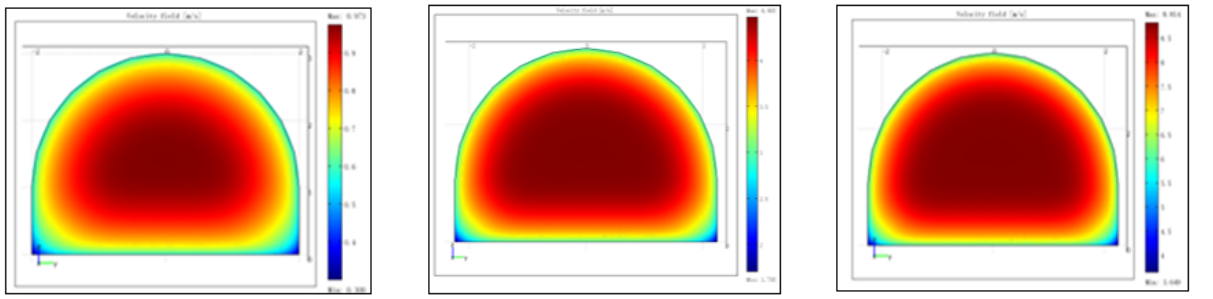

(a)Entrance wind speed of 0.8m/s (b)Entrance wind speed of 4m/s (c)Entrance wind speed of 8m/s

Figure 5. Contour map of velocity distribution at different inlet wind speeds in a semicircular arch roadway (4.5m×3.3m)

From Figures 4~5, it can be seen that: (1) the contour line of the wind speed contour line of the tunnel section is consistent with the shape of the section, and the wind speed contour line is basically parallel to the tunnel wall. The wind speed contour line expands from the central part of the tunnel section to the tunnel wall. (2) The closer the wind speed contour line is to the wall of the tunnel, the denser it is, indicating that the wind speed gradient is larger near the wall, and the sparser the wind speed contour line is closer to the middle of the tunnel, indicating that the wind speed gradient is smaller and the central wind speed of the tunnel is basically equal. (3) In the same tunnel, the higher the average wind speed, the smaller the thickness of the near wall velocity variation layer, that is, the thickness of the boundary layer decreases with the increase of wind speed.

ISSN: 2688-8645

4.2. Simulation Data Analysis of Wind Speed on the Axis of Each Section of the Tunnel

Based on the section wind speed distribution at X=50m in the tunnel in Chapter 4.1, obtain an empirical calculation formula for calculating the average wind speed of the tunnel section through the wind speed at the tunnel section point. On this basis, use Origin 8.0 to fit non-linear functions of point velocity and average wind speed. According to the simulated scheme, the selected tunnel type is used as the data monitoring location at X=50m of the tunnel, with the central axis of the tunnel as the data monitoring line. Due to space constraints, only the results of a rectangular roadway with a width of 4m × a height of 3m and a semicircular arch roadway with a width of 4.5m × a height of 3.3m are provided.

When the roadway is a rectangular roadway with a width of 4m × a height of 3m, and the inlet wind speeds are 0.8m/s, 2m/s, 4m/s, 6m/s, and 8m/s respectively, the corresponding relationship between point velocity v and distance d can be analyzed. Then, the ratio of the wind speed value v at each point on the central axis to the average wind speed v' on the cross-section of the roadway can be obtained as a function of the distance d between each point on the central axis and the roof, as shown in Table 4.

Table 4. Relationship between v / v' and d under different inlet wind speeds in a rectangular roadway with 4m wide × 3m high

Inlet velocity /m.s^{-1}	The distance between each point on the axis of the tunnel and the roof d/m	The ratio of the wind speed values at each point on the central axis to the average wind speed on the tunnel section v / v'
0.8	$d\subseteq(0,1.25]$	1.1839+0.1633ln$d$
	$d\subseteq[1.25,1.5]$	1.225
2.0	$d\subseteq(0,1.25]$	1.1573+0.1391ln$d$
	$d\subseteq[1.25,1.5]$	1.21
4.0	$d\subseteq(0,1.25]$	1.1406+0.1267ln$d$
	$d\subseteq[1.25,1.5]$	1.185
6.0	$d\subseteq(0,1.25]$	1.1332+0.1189ln$d$
	$d\subseteq[1.25,1.5]$	1.175
8.0	$d\subseteq(0,1.25]$	1.1273+0.1146ln$d$
	$d\subseteq[1.25,1.5]$	1.1663

Similarly, when the roadway is a semicircular arch roadway with a width of 4.5m × a height of 3.3m, the ratio of the wind speed value v at each point on the central axis to the average wind speed v' on the cross-section of the roadway varies with the distance d between each point on the central axis and the roof, as shown in Table 5.

A total of 25 sets of numerical simulation models for rectangular tunnels and semi-circular arch tunnels were established based on the above. According to the simulation results, it can be concluded that: (1) the distribution characteristic map of cross-sectional wind speed is approximately a "flat bottomed pot shape". The contour line of wind speed is basically parallel to the wall of the tunnel. The wind speed gradient near the tunnel wall is large, while the wind speed gradient in the middle of the tunnel is small. The thickness of the boundary layer decreases with increasing wind speed. (2) The ratio of the maximum wind speed to the average wind speed of the tunnel section is about 1.2. The distance between the average wind speed line of a semi-circular arch roadway and the roof is 10.76% to 1.12% of the roadway height,

ISSN: 2688-8645

while the distance between the average wind speed line of a rectangular roadway and the roof is 10.76% to 11.03% of the roadway height. The distance from the position of the average wind speed line in the tunnel to the roof is approximately 11% of the height of the tunnel.

Table 5. Relationship between v / v' and d under different inlet wind speeds in a semicircular arch roadway with 4.5m wide × 3.3m high

Inlet velocity /m.s^{-1}	The distance between each point on the axis of the tunnel and the roof d/m	The ratio of the wind speed values at each point on the central axis to the average wind speed on the tunnel section v / v'
0.8	d⊆(0,1.6]	1.1476+0.1473lnd
	d⊆[1.6,1.65]	1.2
2.0	d⊆(0,1.6]	1.102+0.1038lnd
	d⊆[1.6,1.65]	1.135
4.0	d⊆(0,1.6]	1.0894+0.0908lnd
	d⊆[1.6,1.65]	1.1175
6.0	d⊆(0,1.6]	1.0827+0.084lnd
	d⊆[1.6,1.65]	1.107
8.0	d⊆(0,1.6]	1.0793+0.0806lnd
	d⊆[1.6,1.65]	1.1012

5. Conclusion

(1) The main controlling factors for the distribution of wind speed in tunnels include the shape and size of the tunnel section, the air supply to the tunnel, the quality of the section forming, the form of support, and the internal facilities of the tunnel.

(2) A calculation model for the position of the average wind speed line in rectangular and semicircular arch tunnels was established based on the Boussinesk theory and Prandtl turbulence theory. The general expression for tunnel air volume and the expression for the relationship between the average wind speed line and the tunnel wall were obtained. The position of the average wind speed line in the roadway is only related to the size of the roadway and is not related to other controlling factors.

(3) A total of 25 sets of numerical simulation models for rectangular and semicircular arch tunnels were established, and the distribution characteristics of wind speed on the tunnel section were obtained: the distribution characteristic map of wind speed on the section is approximately a "flat bottomed pot shape". The contour line of wind speed is basically parallel to the wall of the tunnel. The wind speed gradient near the tunnel wall is large, while the wind speed gradient in the middle of the tunnel is small. And the thickness of the boundary layer decreases with increasing wind speed.

(4) The ratio of the maximum wind speed to the average wind speed of the tunnel section is about 1.2. The distance between the average wind speed line of a semicircular arch tunnel and the roof is 10.76% to 1.12% of the tunnel height, while the distance between the average wind speed line of a rectangular tunnel and the roof is 10.76% to 11.03% of the tunnel height. That is, the distance from the average wind speed line position of the tunnel to the roof is approximately 11% of the tunnel height.

ISSN: 2688-8645

Acknowledgments

The study was supported by Tiandi Technology Co., Ltd. Technology Innovation and Entrepreneurship Fund Special Project (2022-2-TD-ZD010) and Key R&D Project of middling coal Science and Engineering Group Chongqing Research Institute Co., Ltd. (2022ZDXM09).

References

[1] Zhang Jinggang, Wang Qingyan, He Xin. The current situation of intelligent ventilation in mines and the construction of intelligent control systems [J]. Mining Safety and Environmental Protection, 2023,50(05): 37-42.

[2] Yuan Liang, Zhang Nong, Kan Jiaguang, et al. Concept, model, and prediction of green coal resources in China [J]. Journal of China University of Mining and Technology, 2018,47(01): 1-8.

[3] Zhang Peisen, Zhang Xiaole, Dong Yuhang, et al. Analysis and prediction of coal mine accidents in China from 2008 to 2021 [J]. Mining Safety and Environmental Protection, 2023,50(02): 136-140+146.

[4] Wang Yungang, Cui Chunyang, Zhang Feiyan, et al. Statistical analysis and research on major and above coal mine accidents in China from 2011 to 2020 [J]. Journal of Safety and Environment, 2023,23(09): 3269-3276.

[5] Zhang Chaolin, Wang Peizhong, Wang Enyuan, et al. 70 year development history and prospects of coal and gas outburst mechanisms in China [J]. Coalfield Geology and Exploration, 2023,51(02): 59-94.

[6] Luo Guang, Zou Yinhui, Ning Xiaoliang, et al. Research and application of online monitoring technology for mine ventilation network [J]. Mining Safety and Environmental Protection, 2019, 46(05): 47-50.

[7] Lu Guangli, Zhang Menghan, Fan Congqi. Analysis of fixed-point wind speed measurement method based on CFD [J]. Coal Technology, 2015,34(05): 156-157.

[8] Zhou Xihua, Meng Le, Li Chengyu, et al. Experimental study on wind speed measurement and correction methods for circular pipelines [J]. Journal of Liaoning University of Engineering and Technology (Natural Science Edition), 2012,31(06): 801-804.

[9] Wang Hanfeng. Simulation study on positioning and monitoring of average wind speed points in tunnel sections based on Fluent [J]. Coal Science and Technology, 2015,43(08): 92-96.

[10] Song Ying, Liu Jian, Li Xuebing, et al. Experimental and simulation research on the distribution law of average wind speed in mine tunnels [J]. China Safety Science Journal, 2016,26(06): 146-151.

[11] Liu Jian, Song Ying, Li Xuebing, et al. Experimental study on the distribution law of sudden expansion wind speed in a straight roadway section based on LDA [J]. Journal of China Coal Society, 2016,41(04): 892-898.

[12] Ding Cui. Numerical and experimental study on the distribution characteristics of average wind speed in trapezoidal tunnels [J]. Journal of Safety Science and Technology, 2016,12(01): 28-32.

[13] Luo Guang Research on the Distribution Law of Wind Speed and Accurate Monitoring of Wind Volume in Typical Tunnel Sections [D]. Beijing: Coal Science Research Institute, 2020.

[14] Hu Jianhua, Zhao Yang, Zhou Tan, et al. Multiple factors affecting the distribution of wind speed on the cross-section of uneven roof tunnels [J] Journal of Central South University, 2021,28(07): 2067-2078.

[15] Shao Liangshan, Wen Shuangshuang. Research on obtaining average wind speed in tunnels based on GRU neural network [J]. Gold Science and Technology, 2021,29(05): 709-718.

[16] Wang Heng, Qiu Liming, He Xueqiu, et al. Research on the distribution law of wind speed at the cross-section of coal mine tunnels under different factors [J]. Mining Research and Development, 2022, 42(07): 125-132.

[17] Zhang Shiling. Underground experimental study on the distribution characteristics of wind speed in tunnel sections [J]. Coal Technology, 2022, 41(08): 119-122.